Flow over Small Heat Islands: A Numerical Sensitivity Study

HANNU SAVIJÄRVI AND STUART MATTHEWS*

Division of Atmospheric Sciences, Department of Physical Sciences, University of Helsinki, Helsinki, Finland

(Manuscript received 30 September 2002, in final form 19 May 2003)

ABSTRACT

A two-dimensional nonlinear model with physical parameterizations was applied to simulate the observed diurnal variation on the 5-km-wide flat tropical island of Nauru in the trade wind zone. Both the model and Atmospheric Radiation Measurement (ARM) campaign aircraft observations indicate vigorous mixing in the typical sunny daytime conditions, leading to a warm plume downstream of the island. The model's afternoon wind field displayed rising motion downstream and downwash ahead of the island with gravity wave structure, in accordance with linear models of steady flow over a heated island. The roughness difference between sea and land added local rising motion above the windward coast and sinking motion above the lee.

Without large-scale wind U, a weakish sea-breeze (SB) pattern develops during the day in this model over the 5-km-wide island/peninsula. This pure SB circulation intensifies with increasing island width up to 40 km. When large-scale wind is present, the morning leeside SB cell is advected out to sea and disappears while the windward coast SB cell tilts over the island and is transformed into the steady heat island–type perturbation during the day.

During the night, a reversed heat island–type weak and shallow perturbation develops for nonzero U. For $U = 0$, the sea breeze dies in the evening and no land breeze appears. If a 200-m-high central mountain is added to a 20-km-wide island/peninsula in calm daytime conditions, the SB circulation is enhanced by upslope winds followed by weak katabatic flow down the cool slopes during the night. When any large-scale flow is present, the forced flow up and down the slopes appears to dominate the wind perturbation patterns day and night.

1. Introduction

Three types of island circulation can be identified in the meteorological literature: those associated with large, flat islands; those associated with tall islands; and those associated with small islands. All three types occur within a stable maritime environment. Large islands, such as the Tiwi Islands (Saito et al. 2001) and Puerto Rico (Malkus 1955) mainly appear to generate sea-breeze-assisted convective mesoscale complexes, while tall islands, such as Hawaii (Smith and Grubiac 1993; Reisner and Smolarkiewicz 1994) primarily act as mechanical obstacles on the flow. The circulations associated with small islands (5–40 km in diameter) are perhaps the least well known. Studies of these are briefly summarized in section 2.

We have traced two types of linear analytic models for heat islands. The first is for oscillating land and sea breezes (SBs) with no large-scale wind, such as Defant's (1950; see also Pielke 2002). The second is for steady-state flow over a warm, flat region; these produce a cell of downward motion over the upwind side of the warm region and upward motion over the lee side with upward propagating damped gravity wave features (e.g., Olfe and Lee 1971; Smith and Lin 1982; Lin 1986; Hsu 1987a,b; Baik 1992). Dalu et al. (1996) have combined the two types. However, their results are not reliable for small islands in weak background flow, as the solutions are then in a resonance region between the two types, amplitudes being large and compensating. Here, numerical simulations might be more realistic. Also, linear models have had very simplified turbulence parameterizations and no other physics (no moisture, no radiation, no topographical, roughness, or temporal surface temperature variations).

The U.S. Atmospheric Radiation Measurement (ARM) program has a site on the flat tropical island of Nauru (0.5°S, 166.9°E) in the trade wind zone. During a campaign between 16 June–15 July 1999, meteorological measurements on the 5-km-wide island were augmented by ship observations and aircraft measurements. The campaign and its results will be described in more detail elsewhere. Here, we utilize the ARM observations in validating simulations by a two-dimen-

* Current affiliation: CSIRO Forestry and Forest Products, Hobart, Tasmania, Australia.

Corresponding author address: Prof. Hannu Savijärvi, Division of Atmospheric Sciences, P.O. Box 64, Department of Physical Sciences, University of Helsinki, Helsinki FIN-00014 Finland.
E-mail: hannu.savijarvi@helsinki.fi

sional numerical model with physical parameterizations for the diurnal variation over Nauru. We then investigate the diurnal flow perturbations caused by small islands (or peninsulas) for various island sizes and topographies and for various background flow speeds, having realistic forcing in all cases through the model physics.

2. Small heat island circulations

The wind field above small tropical islands has not been well documented by observations. Garstang et al. (1975) have reviewed the structure of smallish heat islands, summarizing several experiments on Barbados, an island of moderate size (20 km diameter) and relief (220 m) in the tropical Atlantic (trade winds typically 12 m s^{-1}). Daytime aircraft transects revealed a plume of heated and dryish air extending downstream of the island. Linear analytic (Olfe and Lee 1971) and nonlinear numerical (Estoque and Bhumralkar 1969) models of flow over a warm, flat zone also produced such thermal features. Using pilot balloon measurements DeSouza (1972; summarized in Garstang et al. 1975) calculated wind divergences and vertical motions over Barbados. These displayed downward motion over Barbados during the day, upward motion downwind from it, and the reverse at night, in agreement with the flat island linear model predictions of section 1.

Mahrer and Pielke (1976) performed a series of three simulations of Barbados at 5-km horizontal resolution: a three-dimensional model with island topography, 3D without topography, and 2D with topography. They found that in the simulations with topography, the wind was dominated by flow over the topography and that only the 3D simulation without topography resulted in a daytime wind field similar to that described by DeSouza (1972). Mahrer and Pielke argued that the differences between their model results and DeSouza's analysis arose because DeSouza's divergence calculations neglected to account for terrain slope.

As the effect of topography in a 2D model has not been thoroughly investigated (Mahrer and Pielke did not describe a 2D experiment without topography) the relationship between the 2D results and the Barbados observations remains unclear. We will comment on this later based on the present 2D model experiments.

3. The UH model and the Nauru results

Pielke (2002) and Hsu (1987a) have shown that a hydrostatic approach is fairly accurate for heat-island-type flows, for islands larger than about 1 km. We use here the two-dimensional University of Helsinki (UH) mesoscale model, the sigma coordinate dynamical core of which originates from Alpert et al. (1982). The physical parameterizations include a Monin–Obukhov surface layer, mixing length turbulence closure, cloud physics, advanced longwave (LW) and shortwave (SW) radiation schemes and an interactive (force–restore method) soil scheme. A large-scale pressure distribution in the form of constant free-atmosphere large-scale wind U is defined; U can be zero in the calm case. The vertical velocity ($\dot{\sigma}$) vanishes at the ground and at the model top (at 400 mb) while a free flow condition is applied at the horizontal boundaries. The model equations, parameterizations, and details can be found in the references below.

The UH model has been used to study, for example, coastal convergence and sea/land breezes (Alestalo and Savijärvi 1985; Neumann and Savijärvi 1986; Savijärvi and Alestalo 1988; Savijärvi 1995); slope winds and nocturnal jets in the Great Plains (Savijärvi 1991); the complex local winds around tropical Lake Tanganyika (Savijärvi 1997); inland, coastal, and in-valley urban heat island circulations (Savijärvi 1985; Savijärvi and Jin 2001); and flow perturbations caused by heterogeneous landscape (Vihma and Savijärvi 1991; Savijärvi and Amnell 2001). There is also a version for planet Mars (Savijärvi and Siili 1993; Savijärvi 1999). In all these cases the model results have been close to the available observations (for Mars, those from the Viking and Pathfinder landers) and have revealed the dynamics leading to the local flow perturbations induced by the lower boundary conditions.

For Nauru the model parameters were set either to typical values or to the observed values during the ARM campaign, when available. The ocean surface temperature was 28.5°C and roughness length 0.1 mm. The island albedo, emissivity, soil heat capacity, and roughness length for momentum were set to 0.18, 0.98, 12×10^4 J m^{-2} K^{-1}, and 20 cm, respectively, while the roughness length for scalars was 5 cm and soil moisture availability 1%. Based on time-averaged radiosoundings from two ships well outside Nauru, the model was initialized and the prevailing large-scale (trade) wind was set to $U = 10$ m s^{-1} (from the east). The model's horizontal grid length is 0.5 km. There are 132 grid points and 25 sigma levels at the approximate altitudes of 2, 10, 29, . . . , 7400 m above the surface. The island of Nauru is a 5-km-wide, flat, rough land zone in the ocean, across which the trade wind U blows. Experiments for a 20-km-wide or wider islands are made using 2-km grid length (thus preserving 10 grid points for the forcing area), 65×11 points, and model top at 700 mb.

The diurnal cycle from the 2D model was fairly close to the average ARM surface observations on Nauru and on the two ships (Fig. 1). The island observations are from the ARM station on the west coast; model values are taken from the lee coast grid point and from an unperturbed ocean point (10 km upstream of land). Briefly, the island ground temperatures reach 36°C during the sunny afternoons while the near-surface maximum temperature and wind are 30°C and 4 m s^{-1}, respectively, dropping to 26°C and 2 m s^{-1} during the night. Over the ocean, diurnal variation is small and the wind speed and humidity are higher. The model's surface flux-

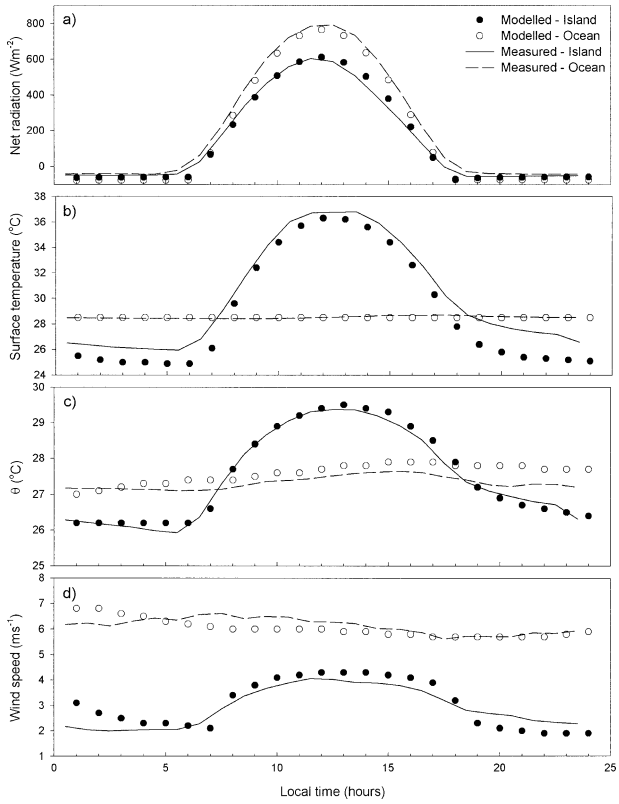

FIG. 1. Diurnal evolution of the observed and modeled near-surface variables over Nauru and the ocean. The observations (curves) are campaign averages from ARM ship (dashed) and land station (thin line) sensors. Model values (circles) are from an upstream ocean grid point and from the leeside island grid point. (a) Net radiation (W m^{-2}); (b) surface temperature (°C); (c) 2-m potential temperature (°C); (d) 10-m wind speed (m s^{-1}).

es of momentum, sensible heat, and latent heat over the sea agreed with those measured at the ships ($\tau = 0.05$ m^2 s^{-2}, $H = 4$ W m^{-2}, LE $= 130$ W m^{-2} on the average, respectively) with deviations below $\pm 2\%$. Also the surface net radiation was well captured by the model (Fig. 1).

The model-produced (upwind) marine boundary layer structure of wind, temperature, and moisture was fairly close to the average ship soundings (Fig. 2) except that the mixed layer was somewhat low for wind and moisture. Soundings were not available over land but aircraft measurements were made during some days. Several legs across the island were flown along and against the trade wind at different altitudes. Both the aircraft observations and the model display vigorous daytime mixing and strong vertical turbulent fluxes over the island. For instance, eddy correlation measurements of sensible and latent heat fluxes produced 200–300 W m^{-2} at 150–200-m altitude above the lee coast at 1400 local time (LT) during the 2 July 1999 flight, while an upward latent heat flux of up to 1000 W m^{-2} was observed at the top of the mixed layer (600 m). These mixing processes lead to a downstream plume of warm and dry air near the surface and in the midmixed layer. The core of this plume was up to 0.3°C warmer and 0.5 g kg^{-1} drier than the marine mixed layer in both the observations and model (differences between the model and observations were within 0.1°C and 0.1 g kg^{-1}). These features are also compatible with linear model results and Barbados observations referred to in sections 1 and 2. The plume extended 20 km downstream in the observations and to the downwind boundary in the model. Near the top of the mixed layer the plume was warm and moist both in the observations and in the UH model, due to the strong mixing. This very turbulent moist upper part of the plume appeared to activate convective clouds occasionally. Unfortunately, there was a partial failure in aircraft wind instrumentation so no direct time-mean wind observations were available for comparison with model results.

The 2D UH model with its physical parameterizations appeared therefore to reproduce the main observed diurnal surface layer and boundary layer structure during the trade wind flow over the small tropical island of Nauru. The results indicate that the daytime 10 m s^{-1} flow over a 5-km flat warm island is within the linear and hydrostatic regime.

4. Sensitivity studies

We will now study numerically the airflow over a smallish flat tropical island/peninsula by varying the geometry and external conditions, mainly the island size and the background wind speed U, but keeping everything else in the model as in the Nauru case of section 3. The forcing should thus remain realistic as it is created in all cases internally by the model's physics. We will concentrate on the horizontal and vertical wind components u and w, as they nicely display the possible sea breeze and convective activities, and allow direct comparison with the linear model results. Some questions to be answered are as follows.

- What is the sea-breeze pattern for various-sized islands when there is no basic flow? Is it weak for a small island? How large an island is needed to reach the mainland sea-breeze strength?
- How does the transformation from a pure sea-breeze pattern into the downstream heat plume pattern take place when the large-scale wind speed is increased?
- What are the nighttime flow patterns as the island then is clearly cooler than the surrounding sea (Fig. 1) and the surface layer must be stable? Is there a land breeze? Does the downstream heat plume disappear or reverse at night?
- What effect does a Barbados-type mountain have on these 2D flows?

a. Daytime breeze development over a flat island

Figure 3 shows the model's w and u' fields for the Nauru case at 1400 LT (island size is 5 km, large-scale

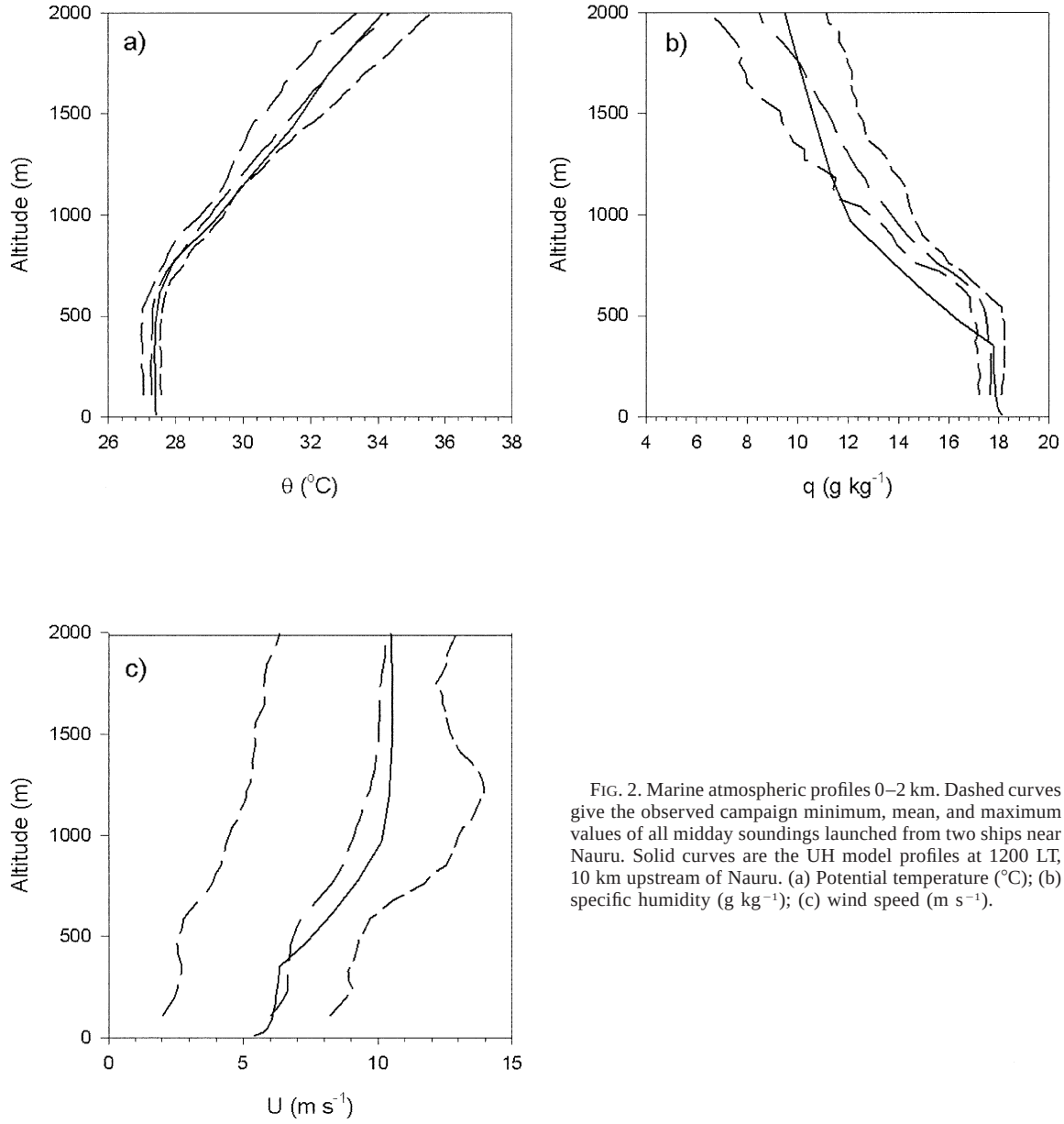

FIG. 2. Marine atmospheric profiles 0–2 km. Dashed curves give the observed campaign minimum, mean, and maximum values of all midday soundings launched from two ships near Nauru. Solid curves are the UH model profiles at 1200 LT, 10 km upstream of Nauru. (a) Potential temperature (°C); (b) specific humidity (g kg^{-1}); (c) wind speed (m s^{-1}).

wind $U = 10$ m s^{-1}). Here, u' is the difference in u from its nonperturbed upstream profile (shown in Fig. 2c); that is, u' is the perturbation pattern caused by the island on the marine background flow. The wind is locally weak (u' is negative) in a shallow layer just above the island. Then u' is positive above the warm island at 100–500 m and negative downwind from the surface to 1500-m altitude, then weakly positive again. This latter pattern leads to rising motion (w: +1–2 cm s^{-1}) in the lee of the island at 1500-m altitude, and to sinking motion (w: −1 cm s^{-1}) at 500-m altitude in front of it. These patterns and the phase tilt in the wind perturbations are of the typical wavelike mode revealed by linear models for steady flow past a heated island. They indicate damped vertical gravity wave propagation set up by the warm surface anomaly.

The strong vertical mixing, together with the rising motion in the lee of the warm island, are conducive to cumulus clouds being initiated there. These afternoon downwind cloud streets are common in Nauru, although they are not formed every day. Their occasional shadows cause the drop in the hourly averaged net radiation on the west coast observations in Fig. 1.

The rising (sinking) motions right above the windward (lee) coast in Fig. 3a are connected with the mechanical roughness change. In order to demonstrate these, Fig. 3c shows the vertical velocity response when the island surface temperature is kept at the sea surface

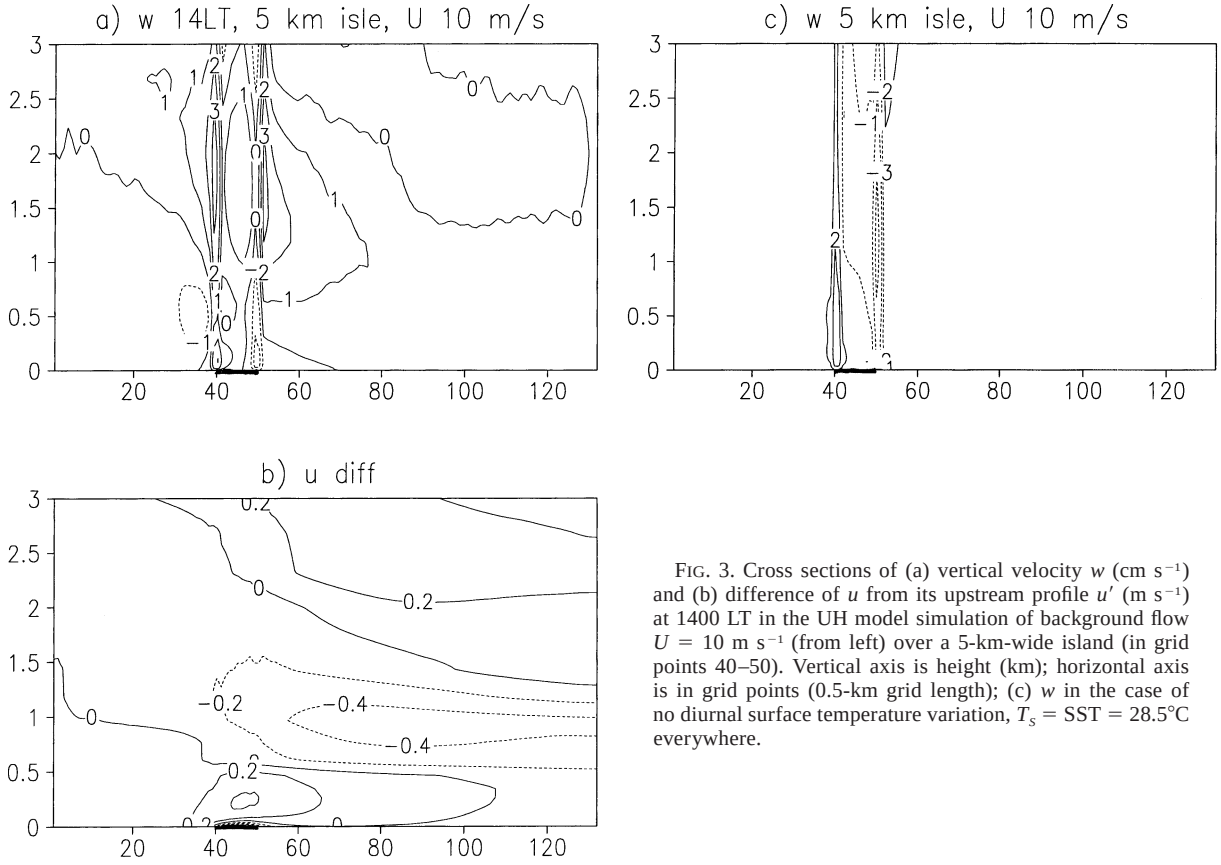

FIG. 3. Cross sections of (a) vertical velocity w (cm s^{-1}) and (b) difference of u from its upstream profile u' (m s^{-1}) at 1400 LT in the UH model simulation of background flow $U = 10$ m s^{-1} (from left) over a 5-km-wide island (in grid points 40–50). Vertical axis is height (km); horizontal axis is in grid points (0.5-km grid length); (c) w in the case of no diurnal surface temperature variation, T_S = SST = 28.5°C everywhere.

temperature; that is, the only mechanism for the perturbation is the surface roughness difference. This leads to the familiar coastal convergence (divergence) and rising (sinking) motion just over the windward (leeside) coast (e.g., Alestalo and Savijärvi 1985). Obviously the other effects seen in Fig. 3a are induced by the evolving thermal contrast between land and sea. Cases with thermal contrast only are shown later in Figs. 6c and 7c.

Figure 4 shows the u and w fields in the Nauru case in the afternoon (at 1400 LT), when there is no large-scale wind in the model ($U = 0$). The symmetric pattern is that of a weakish sea breeze. There is horizontal wind of about 2 m s^{-1} toward the island near the surface 5–10 km out at sea on both sides; return flows of about 1 m s^{-1} aloft at 700-m height, and a narrow joint rising motion pattern above the island center at 400-m height.

With $U = 4$ m s^{-1} the SB pattern is still visible but it is modified by the large-scale advecting wind: The windward coast SB cell is weak and close to the shoreline while the leeside cell is less damped but is advected downstream well over the sea. This is in accordance with the pioneering mainland SB results of Estoque (1962) and Savijärvi and Alestalo (1988).

For $U = 6$ m s^{-1}, shown in Fig. 5, the leeside sea breeze cell has been advected to the model's right boundary by 1400 LT. The weak rising motion connected with it can be traced 20–30 km downstream over the sea at 700-m height. The windward coast SB cell can also be recognized; it is tilted over the island. It has adopted features of steady flow past a heat island; however, the return flow is shifted downstream and there is wave structure with sinking motion in front, and rising motion downstream of the island.

Comparing Figs. 3–5, one can thus note that the steady heat island–type perturbation originates from the windward coast SB cell. This cell cannot proceed inland, as would happen with a mainland sea breeze. Instead, it is phase locked over the warm island and is transformed into the flow-over-an-obstacle-type response during the day with gravity wave propagation features. For Nauru parameters, this appears to take place at around $U = 5$ m s^{-1} in the model. In Savijärvi (1985), a warm coastal city had an analogous ''locking'' effect on the mainland sea breeze at 60°N.

The case of $U = 10$ m s^{-1} over a 20-km-wide island (2-km grid length) is shown in Fig. 6 at 1400 LT. The flow perturbation patterns are qualitatively similar to the 5-km island case (Fig. 3) but they have increased in magnitude. The island near-surface interior temperatures are here slightly higher than on Nauru (by 1°C) as the cooling effect of the inflowing marine air is reduced farther inland. Such warmer daytime temperatures and the related stronger pressure anomalies (''heat lows'') in the interiors of flat tropical islands are dem-

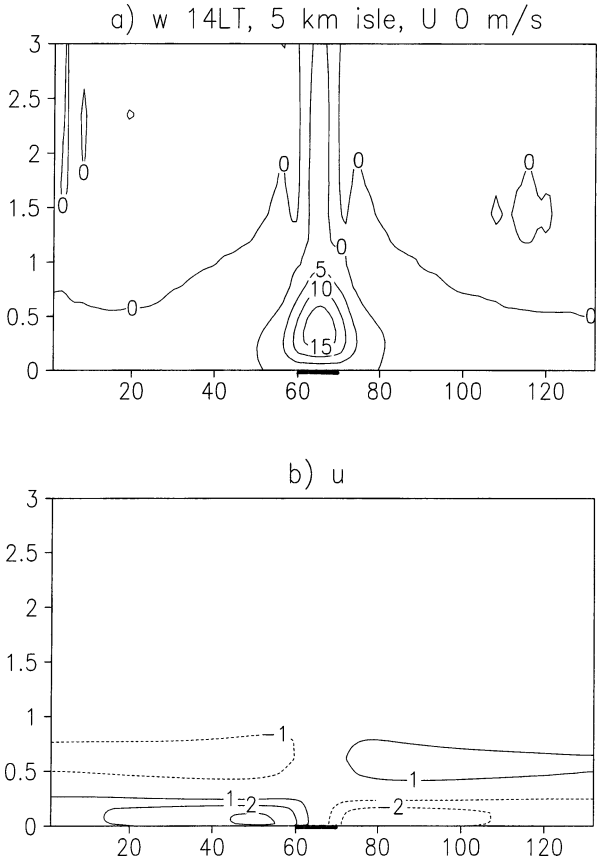

FIG. 4. As Figs. 3a,b but for $U = 0$ and total u instead of u' (5-km-wide island in grid points 60–70). (A sea-breeze pattern.)

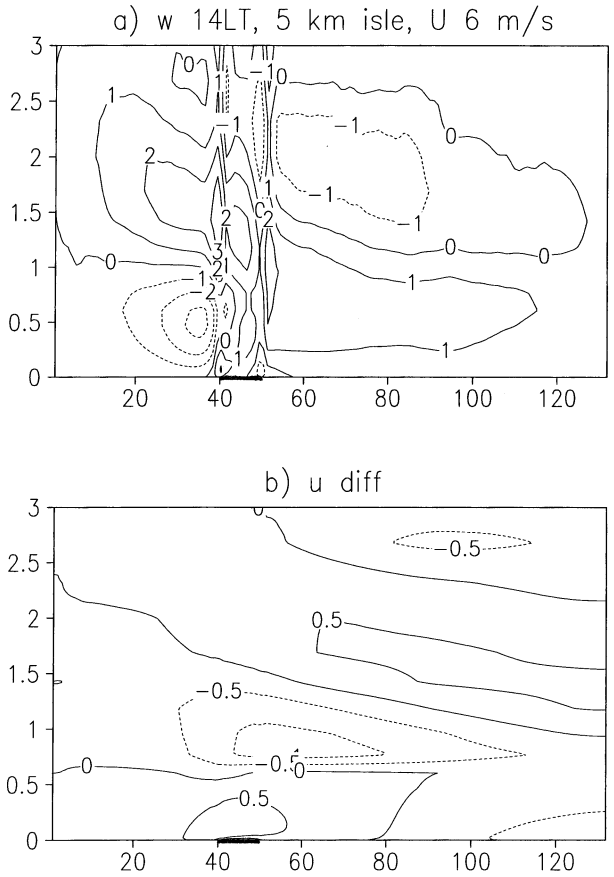

FIG. 5. As in Fig. 4, but for $U = 6$ m s^{-1}.

onstrated, for example, in Oliphant et al. (2001) from observations. Hence, a larger island can pump relatively more heat into the overflowing marine air, thereby increasing the flow response.

Figure 6c shows the vertical velocity pattern from a simplified simulation with heating only. Here, the 20-km-wide island is kept 5 K warmer than SST, the diffusion coefficient of heat K_h is constant (50 m^2 s^{-1}), the diffusion coefficient of momentum $K_m = 0$, radiation and cloud physics are switched off, and the model is run into a steady state. Just above the warm strip u' is, in this case, $+3.5$ m s^{-1} at maximum (due solely to the heat island effect, there being no friction), while it is -1 m s^{-1} aloft. This leads to the familiar pattern in w of Fig. 6c: downwash in front and rising motion above and behind the heat island, not unlike that in Fig. 6a. The discontinuous (but realistic) step function–type surface temperature pattern leads to Gibbs oscillations at the boundaries (as in Olfe and Lee 1971). This amounts to extra sinking motion just above the windward coast, and extra rising motion above the lee coast in Fig. 6c. These are opposite to the vertical velocities induced by the roughness differences (shown in Fig. 3c). Therefore some cancellation between the two effects is to be expected in reality.

Also, for a 20-km-wide island/peninsula, the sea breezes ($U = 0$) are enhanced from their 5-km island values, because the larger island's interior is slightly warmer in the afternoon. At 1400 LT the near-surface breeze maxima 5–10 km out at sea are now 3 m s^{-1}, while the return flow maxima aloft at 1000 m are 1.5 m s^{-1}. For a 40-km-wide island, the model's sea breezes reach speeds of 5–6 m s^{-1} near the surface by 1400 LT. The return flow aloft is 3 m s^{-1} at 1300 m, and the w maximum is here 16 cm s^{-1} at 700-m height above the center of the island. Increasing the island size further did not change the magnitude of the SB circulation: by replacing the island with mainland (everything else being the same), the model produced a typical single tropical sea-breeze cell pattern, where the near-surface breeze was, by 1400 LT, 6 m s^{-1} 5 km out at sea, the return flow was 3 m s^{-1} at 1300 m, and the w maximum was 8 cm s^{-1} 30 km inland at 700 m. This single SB cell traveled slowly inland during the afternoon and evening.

The roughly doubled magnitude of w and its location over the midpoint of the 40-km-wide island as compared with the mainland SB is dictated by the two cells blowing against each other, thus effectively doubling the convergence near the surface and locking it into the center

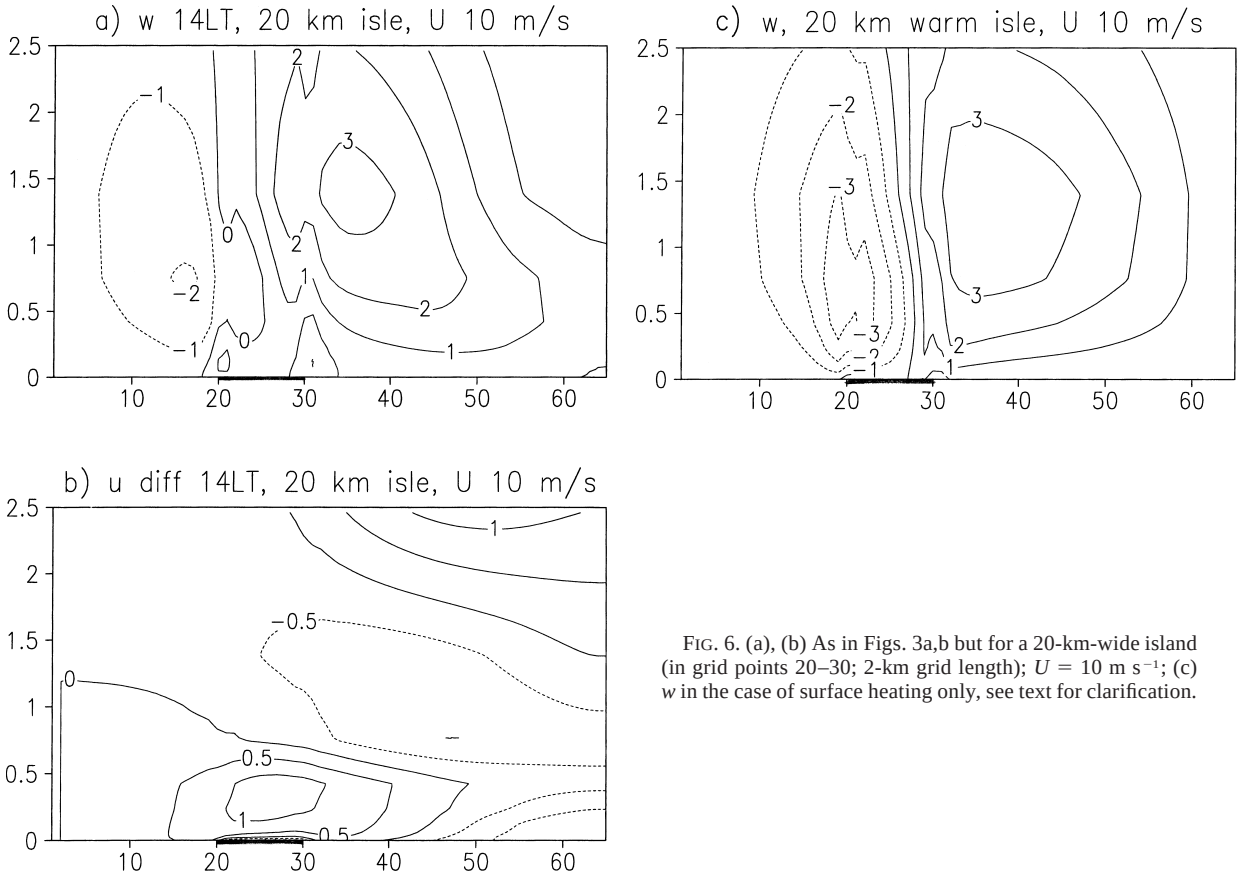

FIG. 6. (a), (b) As in Figs. 3a,b but for a 20-km-wide island (in grid points 20–30; 2-km grid length); $U = 10$ m s^{-1}; (c) w in the case of surface heating only, see text for clarification.

of the island. It is therefore easy to understand that large tropical islands under weak background flow tend to be associated with daytime mesoscale convective complexes triggered by such convergence lines.

It thus appears that the sea breeze of a small island (or peninsula) increases in calm conditions with the island size. It has reached the mainland SB magnitude for a 40–50-km-wide island. This is contrary to linear sea-breeze models. As seen from Table 1, the Defant model with the Martin and Pielke (1983) parameter values produces breezes, which increase in magnitude with decreasing island size, giving quite unrealistic values for small islands (unless friction is increased or the heating amplitude is reduced). The linear steady flow models over a heat source are more realistic in this respect as the temperature advection by the mean wind is included; however, feedback to the fixed surface temperatures and advection by the perturbation is neglected in them.

TABLE 1. Maximum wind component values in the Defant (1950) linear sea-breeze model 8 h after sunrise (1400 LT), with the parameter values from Martin and Pielke (1983) except the island width, which is varied.

Island width (km)	Max u component (m s^{-1}) (at the surface)	Max w component (cm s^{-1}) (at 500 m)
50	6.93	9.51
40	8.08	12.89
30	9.64	18.09
20	11.99	26.32
10	16.82	37.54

b. Nighttime additions

In the case of no background wind, the sea breezes of a tropical island or peninsula die during the evening in our model, and there is practically no wind during the night. This is in accordance with theory and numerical simulations, which show that there is no pure land breeze phase in the Tropics, even if the sea or lake is considerably warmer than land (e.g., Rotunno 1983; Dalu et al. 1996; Yan and Anthes 1987; Savijärvi 1997). The stable nighttime stratification limits vertical diffusion, especially during weak winds, so the temperature difference between warm water and cooler land is not communicated to the air. Hence no thermal circulations develop for $U = 0$ and winds remain weak overnight [cf. Savijärvi and Jin (2001) for an analogous urban heat island circulation case].

The modeled early morning (0600 LT) wind components w and u' for 6 m s^{-1} large-scale wind blowing over a 20-km-wide flat tropical island are shown in Figs. 7a,b. The island is here 3°–4°C cooler overnight than

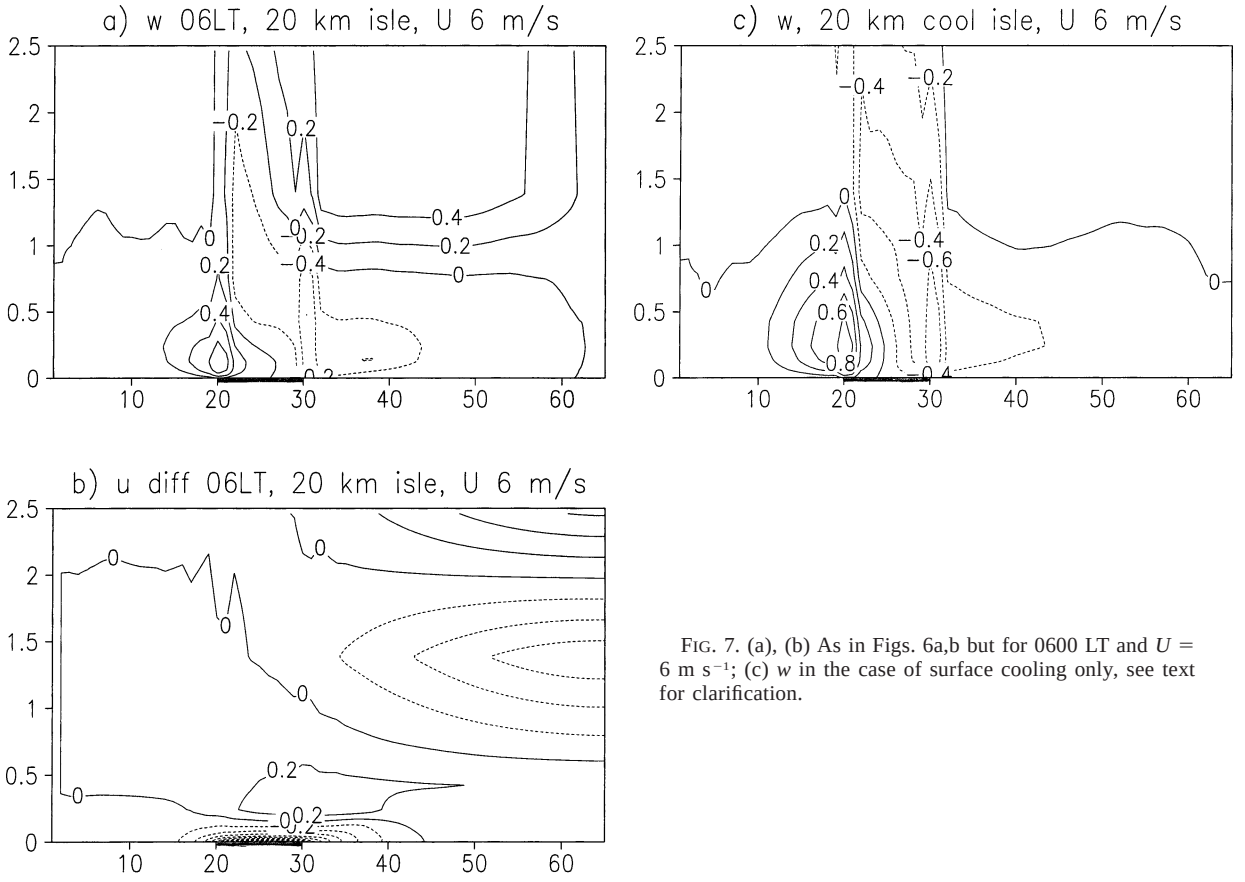

FIG. 7. (a), (b) As in Figs. 6a,b but for 0600 LT and U = 6 m s^{-1}; (c) w in the case of surface cooling only, see text for clarification.

the sea surface (cf. Fig. 1). The flow perturbations are reversed compared with the heat island circulations of section 4a: there is reduced near-surface wind over the cool island, weak rising motion in front and weak sinking motion behind it in a shallow layer.

Figure 7c shows the vertical velocity pattern for steady-state flow over a cool region in the model, mimicking the Figs. 7a,b conditions (T_S = SST − 3 K at the island grid points, $K_h = 5$ m^2 s^{-1}, $K_m = 0$, no radiation, no cloud physics), and opposite to the Fig. 6c conditions. The 6 m s^{-1} wind is now reduced (u' is −1.5 m s^{-1}) just over the island solely by the cool surface (there is no friction), while u' is +0.3 m s^{-1} aloft. Hence, there is rising motion in front and sinking motion above and downstream of the cool island, similarly to the linear model results and to Fig. 7a. The step function–type cold surface temperature anomaly induces Gibbs oscillations at the coastlines with results for w in Fig. 7c, which are opposite to that of a warm strip (Fig. 6c), but similar to those that would be induced by drag differences alone (Fig. 3c). In other words, a cool island renders the mechanical effect of large land drag ineffective.

One may thus summarize that a flat tropical island induces no pure land-breeze-type circulation, and acts, during the night as an antiheat island for overflowing marine air. The resulting wind perturbation is weak and shallow as the driving surface temperature difference (land versus SST) is relatively small, the stable nighttime stratification limits vertical mixing, and the effects of roughness differences are minimized during stable stratification.

c. Topography additions

Figure 8 shows the afternoon (1400 LT) flow field for a 20-km-wide island/peninsula simulation with no basic flow, but now with a 200-m-high central mountain, mimicking Barbados. Here, the sea breeze is slightly enhanced by the daytime upslope wind mechanism. The near-surface breezes are 4 m s^{-1} and the return flows aloft, 2 m s^{-1}, while these values without the mountain were 3 and 1.5 m s^{-1}, respectively, for the pure sea breeze of a similar but flat island (section 4a).

The same 20-km, 200-m-mountain island/peninsula case, but with large-scale wind of 6 m s^{-1} is shown in Fig. 9 for 1400 LT. One may note that the leeside SB pattern is advected well out to the sea. The patterns of vertical motion are dominated by forced rising motion on the windward slope and sinking motion down the lee slope, but rising motion associated with the heat island effect is visible in the lee of the island. If the large-scale wind is much stronger than 6 m s^{-1}, the

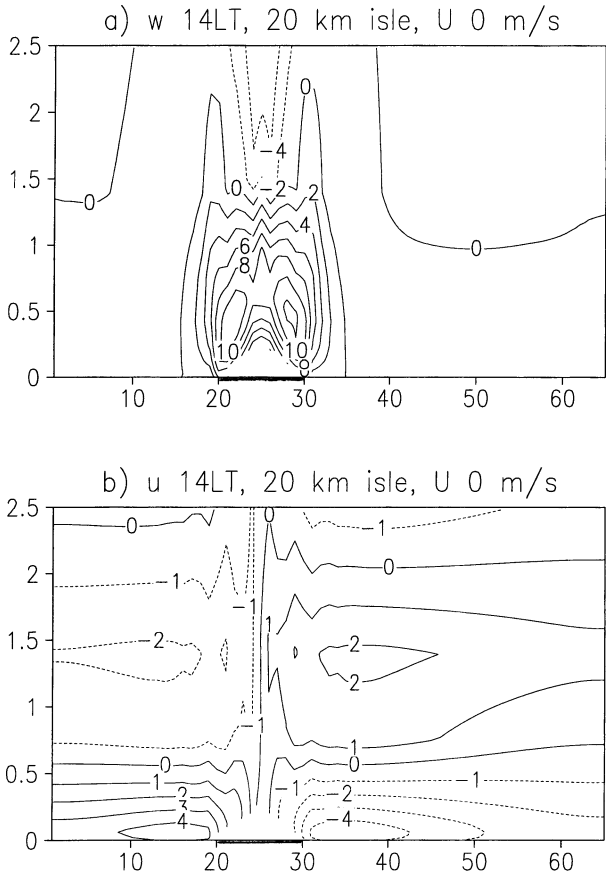

FIG. 8. As in Figs. 6a,b but for $U = 0$, and there is a 200-m-high central mountain on the 20-km-wide island. (Here, sea breezes are combined with upslope flows.)

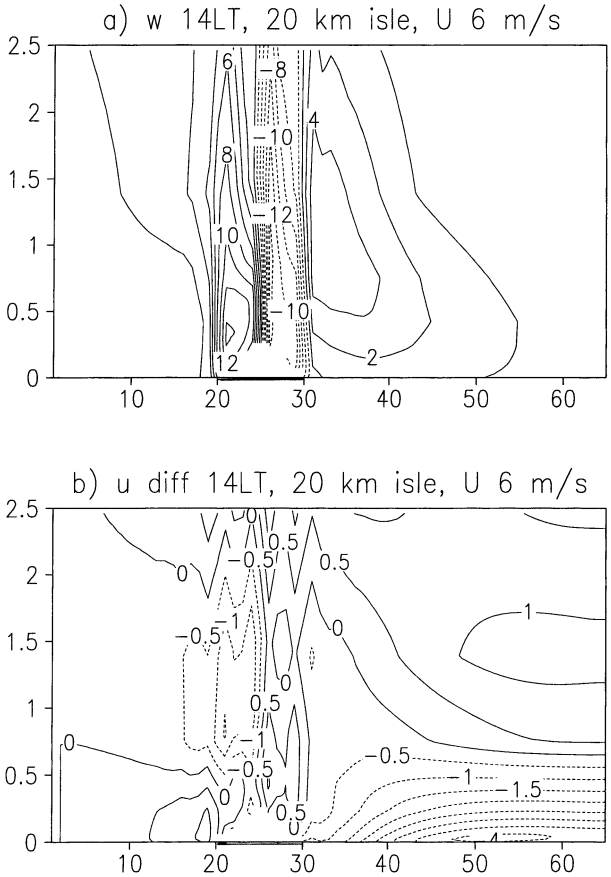

FIG. 9. As in Fig. 8, but $U = 6$ m s^{-1}, and u' is shown.

topographically forced component of the flow will completely dominate in a 2D model. This would be the case for Barbados, where the trade wind speed is typically 12 m s^{-1}, in accordance with the 2D and 3D results of Mahrer and Pielke (1976).

During the night, a 20-km-wide island with a 200-m-high mountain produces in a 2D calm case ($U = 0$) simulation a katabatic flow pattern, where the shallow winds down the cool slopes are, at their maximum, only about 1 m s^{-1} in the model at 0200 LT. This weak thermally/topographically induced pattern is, of course, washed away by moderate maritime background flow. In this case the modeled wind perturbations display the familiar standing gravity wave patterns of stable flow crossing a hill.

5. Concluding remarks

Flow over small tropical islands was studied numerically by simulating the typical observed diurnal variation on the 5-km-wide flat island of Nauru located near the equator in the 10 m s^{-1} easterly trade wind zone. An ARM tropical site campaign provided surface observations, ship soundings and aircraft transects. The UH nonlinear 2D model with physical parameterizations reproduced the available observations fairly well at 0.5-km horizontal resolution. Both the model and the aircraft observations indicate vigorous mixing in the typical sunny daytime conditions leading to a warm plume downstream of the island with occasional cumulus cloud streets. The model's afternoon wind field displayed rising motion downstream and downwash in front of the island/peninsula with gravity wave signature, in accordance with linear models of steady flow over a heat source. Mechanical roughness difference between sea and land added localized rising motion just above the windward coast and sinking motion above the lee.

Sensitivity tests were made varying the setup. When the large-scale trade wind U is removed, a sea-breeze-type pattern develops during the day over the small, flat tropical island. This pure SB circulation intensifies in the model with increasing island/peninsula size up to 40-km width as a broader peninsula can load relatively more heat into the overflowing cool marine air. When weak to moderate large-scale wind is introduced, the morning leeside SB cell is advected out to sea and disappears while the windward coast cell locks over the island and is transformed into the steady heat island–type perturbation. For Nauru, the transition from SB to

a steady flow-type perturbation pattern would appear to take place at around $U = 5$ m s^{-1} in the model.

During the night, a reversed heat island–type weak and shallow wind perturbation develops in the case of large-scale flow over a cool flat island, while in calm conditions, the sea breeze dies in the evening and no land breeze appears. If a 200-m-high central mountain is added to a 20-km-wide island (mimicking Barbados, for instance), in calm daytime conditions the sea-breeze circulations are enhanced by upslope winds, followed by weak katabatic flows down the cool slopes during the night. When large-scale flow is present, the forced flow up and down the slopes dominates the wind patterns in the model, and certainly so for $U = 12$ m s^{-1} typical of Barbados.

One may ask what difference a 3D model would make. The results of Hsu (1987b) for steady linear 3D flow over a heat source indicate that, for a flat circular source, there is not much difference to the 2D solution, but for an elongated heat source, the end point horizontal curvatures of the heat source force two or more cell structures there. Nauru is a roughly circular, flat island. The main difference between our 2D simulations and the aircraft observations was that the warm plume extended farther downstream in the model than in the observations. We believe that this is due to the 3D effect that the perturbation is weaker on the sides of a circular island compared to the centerline. This may weaken the whole plume (through horizontal mixing, for instance). For a nonflat island, a 3D model is clearly needed.

Acknowledgments. The ARM data were obtained from the Atmospheric Radiation Measurement Program sponsored by the U.S. Department of Energy, Office of Science, Office of Biological and Environmental Research, Environmental Sciences Division. S. M. acknowledges support from CIMO, Finland, without which the work would not have been possible. The calculations were made at the Center for Scientific Computing (CSC), Espoo, Finland.

REFERENCES

Alestalo, M., and H. Savijärvi, 1985: Mesoscale circulations in a hydrostatic model: Coastal convergence and orographic lifting. *Tellus,* **37A,** 156–162.

Alpert, P., A. Cohen, E. Doron, and J. Neumann, 1982: A model simulation of the summer circulation from the eastern Mediterranean past Lake Kinneret in the Jordan Valley. *Mon. Wea. Rev.,* **110,** 994–1006.

Baik, J.-J., 1992: Response of a stably stratified atmosphere to low-level heating—An application to the heat island problem. *J. Appl. Meteor.,* **31,** 291–303.

Dalu, G. A., R. A. Pielke, M. Baldi, and X. Zeng, 1996: Heat and momentum fluxes induced by thermal inhomogeneities with and without large-scale flow. *J. Atmos. Sci.,* **53,** 3286–3302.

Defant, F., 1950: Theorie der land- und seewind. *Arch. Meteor. Geophys. Bioklimatol.,* **A2,** 404–425.

DeSouza, R. L., 1972: A study of atmospheric flow over a tropical island. Ph.D. thesis, Dept. of Meteorology, The Florida State University, 203 pp.

Estoque, M. A., 1962: The sea breeze as a function of the prevailing synoptic situation. *J. Atmos. Sci.,* **19,** 244–250.

——, and C. M. Bhumralkar, 1969: Flow over a localized heat source. *Mon. Wea. Rev.,* **97,** 850–859.

Garstang, M., P. D. Tyson, and P. D. Emmitt, 1975: The structure of heat islands. *Rev. Geophys. Space Phys.,* **11,** 139–165.

Hsu, H.-M., 1987a: Study of linear steady atmospheric flow above a finite surface heating. *J. Atmos. Sci.,* **44,** 186–199.

——, 1987b: Mesoscale lake-effect snowstorms in the vicinity of Lake Michigan: Linear theory and numerical simulations. *J. Atmos. Sci.,* **44,** 1019–1040.

Lin, Y.-L., 1986: Calculation of airflow over an isolated heat source with application to the dynamics of V-shaped clouds. *J. Atmos. Sci.,* **43,** 2736–2751.

Mahrer, Y., and R. A. Pielke, 1976: Numerical simulation of airflow over Barbados. *Mon. Wea. Rev.,* **104,** 1392–1402.

Malkus, J. S., 1955: The effects of a large island upon the trade-wind air stream. *Quart. J. Roy. Meteor. Soc.,* **81,** 538–550.

Martin, C. L., and R. A. Pielke, 1983: The adequacy of the hydrostatic assumption in sea breeze modeling over flat terrain. *J. Atmos. Sci.,* **40,** 1472–1481.

Neumann, J., and H. Savijärvi, 1986: The sea breeze on a steep coast. *Beitr. Phys. Atmos.,* **59,** 375–389.

Olfe, D. B., and R. L. Lee, 1971: Linearized calculations of urban heat island convection effects. *J. Atmos. Sci.,* **28,** 1374–1388.

Oliphant, A. J., A. P. Sturman, and N. J. Tapper, 2001: The evolution and structure of a tropical island sea/land-breeze system, northern Australia. *Meteor. Atmos. Phys.,* **78,** 45–59.

Pielke, R. A., 2002: *Mesoscale Meteorological Modelling.* 2d ed. Academic Press, 672 pp.

Reisner, J. M., and P. K. Smolarkiewicz, 1994: Thermally forced low Froude number flow past three-dimensional obstacles. *J. Atmos. Sci.,* **51,** 117–133.

Rotunno, R., 1983: On the linear theory of the land and sea breeze. *J. Atmos. Sci.,* **40,** 1999–2009.

Saito, K., T. Keenan, G. Holland, and K. Puri, 2001: Numerical simulation of the diurnal evolution of tropical island convection over the maritime continent. *Mon. Wea. Rev.,* **129,** 378–400.

Savijärvi, H., 1985: The sea breeze and urban heat island in a numerical model. *Geophysica,* **21,** 115–126.

——, 1991: The U.S. Great Plains diurnal ABL variation and the nocturnal low-level jet. *Mon. Wea. Rev.,* **119,** 833–840.

——, 1995: Sea breeze effects on large-scale atmospheric flow. *Contrib. Atmos. Phys.,* **68,** 335–344.

——, 1997: Diurnal winds around Lake Tanganyika. *Quart. J. Roy. Meteor. Soc.,* **123,** 901–918.

——, 1999: A model study of the atmospheric boundary layer in the Mars Pathfinder lander conditions. *Quart. J. Roy. Meteor. Soc.,* **125,** 483–493.

——, and M. Alestalo, 1988: The sea breeze over a lake or gulf as the function of the prevailing flow. *Beitr. Phys. Atmos.,* **61,** 98–104.

——, and T. Siili, 1993: The Martian slope winds and the nocturnal PBL jet. *J. Atmos. Sci.,* **50,** 77–88.

——, and T. Amnell, 2001: Horizontal variability in the wintertime boreal boundary layer: High resolution flight observations and numerical simulations. *Theor. Appl. Climate,* **70,** 245–252.

——, and L.-Y. Jin, 2001: Local winds in a valley city. *Bound.-Layer Meteor.,* **100,** 301–319.

Smith, R. B., and Y.-L. Lin, 1982: The addition of heat to a stratified airstream with application to the dynamics of orographic rain. *Quart. J. Roy. Meteor. Soc.,* **108,** 353–378.

——, and V. Grubiac, 1993: Aerial observations of Hawaii's wake. *J. Atmos. Sci.,* **50,** 3728–3750.

Vihma, T., and H. Savijärvi, 1991: On the effective roughness length over heterogeneous terrain. *Quart. J. Roy. Meteor. Soc.,* **117,** 399–408.

Yan, H., and R. A. Anthes, 1987: The effect of latitude on the sea breeze. *Mon. Wea. Rev.,* **115,** 936–956.